Molecular Motions in Amorphous Ibuprofen As Studied by Broadband Dielectric Spectroscopy

Ana R. Brás,[†] João P. Noronha,[†] Alexandra M. M. Antunes,[†] Maria M. Cardoso,[†] Andreas Schönhals,[‡] Frédéric Affouard,[§] Madalena Dionísio,[†] and Natália T. Correia*[,†]

Requimte, Departamento de Química, Faculdade de Ciências e Tecnologia, Universidade Nova de Lisboa, 2829-516 Caparica, Portugal, Federal Institute of Materials Research and Testing (BAM), Unter den Eichen 87, D-12205 Berlin, Germany, and Laboratoire de Dynamique et Structure des Matériaux Moléculaires, UMR CNRS 8024, UFR de Physique, BAT P5, Université des Sciences et Technologies de Lille, 59655 Villeneuve d'Ascq, France

Received: May 7, 2008; Revised Manuscript Received: June 13, 2008

The molecular mobility of amorphous ibuprofen has been investigated by broadband dielectric relaxation spectroscopy (DRS) covering a temperature range of more than 200 K. Four different relaxation processes, labeled as α, β, γ, and D, were detected and characterized, and a complete relaxation map was given for the first time. The γ-process has activation energy $E_a = 31$ kJ·mol^{-1}, typical for local mobility. The weak β-relaxation, observed in the glassy state as well as in the supercooled state was identified as the genuine Johari−Goldstein process. The temperature dependence of the relaxation time of the α-process (dynamic glass transition) does not obey a single VFTH law. Instead two VFTH regimes are observed separated by a crossover temperature, $T_B = 265$ K. From the low temperature VFTH regime, a $T_g^{diel}{}_{(\tau = 100\ s)} = 226$ K was estimated, and a fragility or steepness index $m = 93$, was calculated showing that ibuprofen is a fragile glass former. The D-process has a Debye-like relaxation function but the temperature dependence of relaxation time also follows the VFTH behavior, with a Vogel temperature and a pre-exponential factor which seem to indicate that its dynamics is governed by the α-process. It has similar features as the Debye-type process observed in a variety of associating liquids, related to hydrogen bonding dynamics. The strong tendency of ibuprofen to form hydrogen bonded aggregates such as dimers and trimers either cyclic or linear which seems to control in particular the molecular mobility of ibuprofen was confirmed by IR spectroscopy, electrospray ionization mass spectrometry, and MD simulations.

1. Introduction

Ibuprofen is a nonsteroidal worldwide used pharmaceutical compound which belongs to the category of 2-arylpropanoic acid (see Scheme 1 in the Experimental and Computer Simulation Details section), showing analgesic, antipyretic and anti-inflammatory properties.[1] Recently, it was found by Johari et al.[2] that the crystallization of ibuprofen can be easily circumvented on cooling from the melt. Then it exhibits similar properties as conventional glass forming materials,[3−5] both in the glassy state and the supercooled liquid.

The knowledge of the time scales and temperature dependences of molecular motions are particularly relevant not only from a fundamental point of view regarding the current interest on glass formers and the glass transition[5−7] but also to profit from the advantageous properties of the amorphous state. Amorphous pharmaceutical compounds can play a crucial role concerning the therapeutic activity. In fact, a growing interest is devoted to the development of amorphous solid pharmaceuticals since the amorphous form of a drug often shows an improved solubility, accelerated dissolution and bioavailability promoting therapeutic activity when compared to the ordered crystalline material as underscored in recent publications.[7−9] However, the amorphous solid state is out of equilibrium, and therefore unstable. If the molecular motions causing this instability are not arrested over a time scale meaningful for pharmaceutical applications, important changes in some of the physicochemical properties[9−11] of the drug can occur. Indeed, significant molecular mobility can persist in the glassy state (below the glass transition temperature, T_g) enabling, for instance, the occurrence of phase transitions such as crystallization.[12,13] In this context, the knowledge of the parameters that characterize the molecular dynamics is important for a stable storage and the shelf life of amorphous pharmaceuticals.[14]

For conventional glass formers the temperature dependence of the relaxation time for the structural relaxation (dynamic glass transition, α-relaxation) in the supercooled state usually shows a deviation from the Arrhenius behavior following the well-known Vogel−Fulcher−Tammann−Hesse law (equation 6 in the Discussion) close to T_g. Recently it was proven that the same phenomenology apply to the dynamical behavior of pharmaceutical compounds.[15−22] The deviation from an Arrhenius behavior provides a useful classification of glass formers.[23−25] Materials are called "fragile" if their temperature dependence of relaxation times markedly deviates from the Arrhenius behavior and "strong" if it is close to the latter. In other words, "fragility" indicates how strongly the relaxation time changes as T_g is approached from temperatures above the glass transition. It is one central parameter describing glassy dynamics and

* To whom correspondence should be addressed. E-mail: n.correia@dq.fct.unl.pt.

[†] Requimte, Departamento de Química, Faculdade de Ciências e Tecnologia, Universidade Nova de Lisboa.

[‡] Federal Institute of Materials Research and Testing (BAM).

[§] Laboratoire de Dynamique et Structure des Matériaux Moléculaires, UMR CNRS 8024, UFR de Physique, BAT P5, Université des Sciences et Technologies de Lille.

10.1021/jp8040428 CCC: $40.75
Published on Web 08/08/2008

reflecting the stability of a liquid structure to temperature changes in the supercooled state.[4]

Broadband dielectric relaxation spectroscopy (DRS) is a powerful tool to probe the molecular dynamics in the supercooled and glassy state[26] and was recently employed in pharmaceutical research.[15−22,27] Since studies about the molecular dynamics of ibuprofen are scarce in the literature,[2] dielectric spectroscopy is applied to get relevant information regarding its different molecular fluctuations from the molten down to the glassy state. A better understanding of the mechanisms of molecular mobility which can cause changes during processing or even storage and handling of pharmaceutical substances is given. Both a wide temperature (143 to 363 K) and frequency range (10^{-1} to 10^{9} Hz) is employed, allowing to provide a complete relaxation map which includes besides the α-process already discussed by Johari et al.,[2] two secondary relaxations (β and γ), and a Debye-type process known for alcohols.[28] The study enables the characterization of ibuprofen without a partial crystallization as it is reported in ref 2. The DRS investigations were complemented with differential scanning calorimetry (DSC), high-performance liquid chromatography (HPLC), electrospray ionization mass spectrometry, infrared spectroscopy (IR) experiments, and molecular dynamics (MD) simulation in order to gain deeper insights into the molecular dynamics, molecular structure, and the hydrogen bonding (HB) statistics of ibuprofen.

2. Experimental and Computer Simulation Details

Materials. Ibuprofen ((2*R*,*S*)-2[4-(2-methylpropyl)phenyl] propanoic acid, $C_{13}H_{18}O_2$ (see Scheme 1)) was purchased from Sigma (catalogue number I4883 (CAS 15687−27−1), lot number 026H1368, 99.8% GC assay) with a molar mass of 206.28 g.mol^{-1} (being a racemic mixture of *S*-(+)-ibuprofen and *R*-(−)-ibuprofen). It was used without further purification. For the sake of simplicity, the studied (±)-ibuprofen mixture will be referred to here as ibuprofen.

Differential Scanning Calorimetry. A 2920 MTDSC TA Instruments calorimeter interfaced with a liquid nitrogen cooling accessory was used for the differential scanning calorimetry (DSC) experiments. Dry high-purity He gas with a flow rate of 30 cm^3/min was purged through the sample. The baseline was calibrated scanning the temperature range of the experiments with an empty pan. The temperature calibration was performed taking the onset of the endothermic melting peak of several calibration standards.[29] A sample of 4.03 mg was introduced in an aluminum pan and hermetically sealed using an encapsulating press. A temperature range from 173 to 353 K was covered using a heating/cooling rate of 5 K/min.

Dielectric Relaxation Spectroscopy. ***Low Frequency Range.*** The complex dielectric function $\varepsilon^*(f) = \varepsilon'(f) - i\varepsilon(f)$ (f = frequency, ϵ' = real part, ϵ'' = imaginary part) was measured by an Alpha-N analyzer from Novocontrol GmbH, covering a frequency range from 10^{-1} Hz to 1 MHz. Approximately 75 mg of the as-received ibuprofen powder with silica spacers of 50 μm thickness was placed between two gold plated electrodes (diameter 20 mm) of a liquid parallel plate capacitor. This cell is sealed and so the evaporation of ibuprofen during successive runs[30,31] is avoided. For the analysis of the thermal transitions the measurements were performed with ibuprofen as a disk prepared by compressing approximately 40 mg under a pressing force of ∼50 kN, placed between two gold plated electrodes (diameter 10 mm).

In order to investigate the molecular mobility in the melt, the supercooled liquid and the glassy state, the sample was kept ∼1 h at 353 K, slightly above T_m, to ensure a complete melting. Dielectric spectra were collected isothermally from $T = 353$ K to $T = 143$ K decreasing the temperature in different steps: in the range 353 K ≥ T ≥ 283 K in steps of 5 K; from 283 to 223 K in steps of 1 K and in the remaining temperature range (223 K ≥ T ≥ 143 K) in steps of 2 K. In addition, to reveal cold crystallization ε^* was measured with increasing temperature from 143 K up to 353 K. A detailed study will be reported elsewhere.

SCHEME 1: Chemical structure of Ibuprofen Molecule, Where C* Is a Chiral Carbon Atom

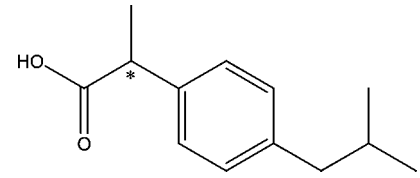

High Frequency Range. From 10^6 Hz to 10^9 Hz a coaxial line reflectometer was employed based on the impedance analyzer HP 4191A. Samples were prepared in parallel plate geometry between two gold-plated electrodes of 6 mm diameter separated by silica spacers of 50 μm thickness. Isothermal frequency scans were carried out from 363 K down to 243 K, in steps of 2 K.

For both frequency regimes, the temperature of the sample was controlled by a Quatro Novocontrol cryo-system with high temperature stability.

Data Analysis. The dielectric spectra were analyzed by fitting a sum of Havriliak-Negami model functions[32] to the isothermal data

$$\varepsilon^*(\omega) = \varepsilon_\infty + \sum_k \frac{\Delta\varepsilon_k}{[1 + (i\omega\tau_{HNk})^{\alpha_{HNk}}]^{\beta_{HNk}}} \qquad (1)$$

where k sums over the different relaxation processes, ω is the angular frequency $\omega = 2\pi f$, τ_{HN} is a characteristic relaxation time that is related to the frequency of maximal loss f_{max}, $\Delta\varepsilon$ is the dielectric relaxation strength of the process under investigation and ε_∞ the high frequency limit of the real part $\varepsilon'(\omega)$; α_{HN} and β_{HN} are fractional shape parameters ($0 < \alpha_{HN} \leq 1$ and $0 < \alpha_{HN}.\beta_{HN} \leq 1$) describing the symmetric and asymmetric broadening of the dielectric spectrum. Conductivity effects were taken into account for temperatures higher than 258 K by adding a contribution ($\sigma_{DC}/\varepsilon_0\omega$) to the imaginary part of the fit function; σ_{DC} is the dc conductivity of the sample and ε_0 is the dielectric permittivity of vacuum.

From the estimated values of τ_{HN}, α_{HN}, and β_{HN}, a model-independent relaxation time τ ($\tau = \tau_{max} = 1/(2\pi f_{max})$) was calculated according to[33]

$$\tau = \tau_{HN} \times \left[\sin\left(\frac{\alpha_{HN}\pi}{2+2\beta_{HN}}\right)\right]^{-1/\alpha_{HN}} \left[\sin\left(\frac{\alpha_{HN}\beta_{HN}\pi}{2+2\beta_{HN}}\right)\right]^{1/a_{HN}} \qquad (2)$$

The analysis of dielectric data was extended by the isochronal representation of the dielectric loss, i.e., ε'' versus temperature at constant frequencies ($\varepsilon''(T, f = \text{const})$). A superposition of k Gaussians[34] was fitted to the isochronal representation of ε'' to obtain the maximum temperature of peaks, $T_{max,k}$, for each measured frequency.

High-Performance Liquid Chromatography. The chemical stability of ibuprofen recrystallized from melt after being kept 1 h at 353 K was determined by high-performance liquid chromatography (HPLC) in comparison with the chromatogram obtained for ibuprofen as received.

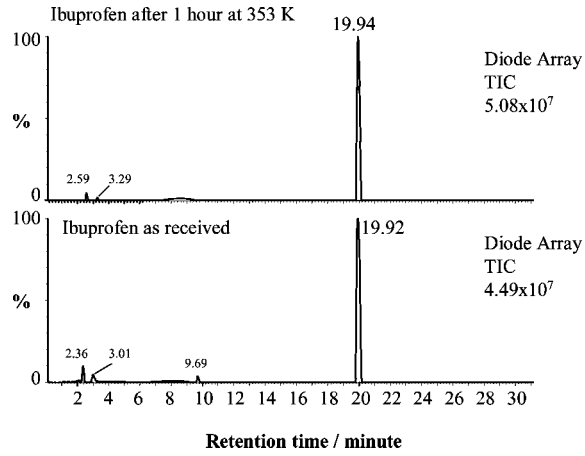

Figure 1. HPLC chromatogram (total ion current (TIC) versus retention time) of ibuprofen dissolved in methanol with a concentration of around $4-5 \times 10^{-4}$ mol/L. Key: ibuprofen as received, bottom chromatogram; ibuprofen recrystallized from the melt after being annealed at 353 K for 1 h, top chromatogram.

HPLC analysis were carried out with a HPLC system (Waters) coupled with a pump and a controller (Waters 600), an in-line degasser (Waters), an autosampler (Waters 717 plus) and a photodiode array detector (DAD, Waters 996). The HPLC analysis was performed in a reverse phase column (Purosphere RP-18e, 250 × 4 mm, 5 μm, Merck) with DAD detection from 200 to 600 nm with a flow rate of 1.0 mL/min, using a 20 min linear gradient from 15 to 100% acetonitrile in formic acid (0.1%), both HPLC grade, followed by a 10 min isocratic elution with acetonitrile. The two analyzed samples (ibuprofen as received and the one obtained after thermal treatment) were dissolved in methanol (HPLC grade).

Only one sharp peak with retention time of 19.93 ± 0.02 min is detected for both samples of ibuprofen as received and annealed at 353 K during 1 h (Figure 1). This proves that the thermal treatment does not affect chemically the ibuprofen structure.

Electrospray Ionization Mass Spectrometry. Electrospray Ionization Mass Spectrometry (ESI-MS) experiments were performed in a quadropole VG Platform (Micromass, U.K., Ltd., MassLynx software version 4.0) spectrometer equipped with an electrospray ionization source operating in the negative ionization mode. Ibuprofen dissolved in methanol (HPLC grade) was infused by a syringe pump (pump 22, Harvard Instruments, USA) with a flow rate of 10 μL/min. Capillary temperature was kept constant between 373 and 393 K. A capillary voltage of 3.5 kV was used. The data were acquired at a constant cone voltage ranging from −20 V to −100 V (in steps of 10 V).

Nitrogen at room temperature was used as drying and nebulizing gas at 300 and 10 mL/min, respectively. The used spectra m/z range was 200−650.

Infrared Spectroscopy. Infrared spectra of both (i) KBr pellet containing an aliquot of ibuprofen recrystallized after being kept 1 h at 353 K and (ii) a drop of neat ibuprofen cooled from the melt inserted between NaCl windows, were recorded, at room temperature, using an ATI Mattson Genesis Series Fourier transform infrared spectrometer. Spectra were taken with a resolution of 4 cm^{-1}; 64 scans were averaged.

Computer Simulation. Molecular Dynamics simulations of a racemic mixture of ibuprofen molecules have been performed using the DL POLY program.[35] The all-atom general amber force field (GAFF)[36] has been used. The starting structure of the *R* and *S* enantiomers was obtained from neutron diffraction of crystalline racemic ibuprofen.[37] The initial configuration of the system was constructed from a 50:50 mixture of each ibuprofen enantiomer randomly located and oriented in a cubic simulation box. The total number of molecules is $N = 54$. The lengths of all covalent bonds were kept fixed using the SHAKE algorithm,[38] with a relative tolerance of 10^{-8}. One fs was used as integration time-step for the equations of motion using the Verlet leapfrog algorithm.[39] A cutoff radius of 12 Å was used to calculate the van der Waals interactions by a Lennard-Jones potential. Lorentz−Berthelot mixing-rules were employed for the cross-interaction terms. Atomic charges were derived from *ab initio* density functional calculation with the B3LYP/6-31G* basic set using the Gaussian package.[40] Electrostatic interactions were handled by the reaction field method using a value of the dielectric permittivity $\varepsilon_{RF} = 8$. The validity of the reaction field method was checked by performing one MD simulation using Ewald summation. No significant structural or dynamical difference has been found between both techniques. A calculation of the average dipole moment yields to a value of ≃1.64 D in agreement with the one reported in the literature for an isolated ibuprofen molecule.[41]

Temperature and pressure have been controlled using the Berendsen thermostat and barostat[42] with a relaxation time of 0.2 and 2.0 ps respectively. The average volume of the simulation box was calculated from constant pressure simulation. The estimated volume has been fixed in the subsequent production simulations, from which all the properties were determined. An experimental value of the density of liquid ibuprofen is not available in the literature. The crystalline structure, the melting enthalpy, the position of the first sharp diffraction peak of ibuprofen in the liquid state and its characteristic relaxation time were well reproduced by this model assuming a density of 0.96 g/cm^3 in the simulations. A detailed discussion will be reported elsewhere. All data reported in the following have been obtained for liquid ibuprofen at 360 K.

3. Results and Discussion

3.1. Association of Ibuprofen Molecules by Hydrogen Bonding. ***Electrospray Ionization Mass Spectrometry.*** Electrospray ionization mass spectrometry was used as a complementary analytical tool in order to investigate the tendency of ibuprofen to form molecular aggregates. Figure 2 shows the mass spectra due to the ionization of ibuprofen (Ibu) obtained for two cone voltages: (a) −20 and (b) −40 V. The intensities of the peaks depend on the ionization conditions. The most probable ions, under these conditions, are: the deprotonated monomer, $[Ibu - H]^-$, which is the one that presents the highest intensity, a homogeneous dimer species, $[2Ibu - H]^-$; and two sodium bridged adducts, $[2Ibu - 2H + Na]^-$ and $[3Ibu - 2H + Na]^-$, respectively, involving two and three ibuprofen molecules.

In electrospray ionization, the analytes in solution are transferred to the gas-phase in a soft manner. Only a low fragmentation of the molecules occurs under controlled operating conditions (in particular, the cone voltage). This is also true for molecular aggregates that already exist in the solution which can be preserved during the ESI process.[43,44] Thus noncovalent aggregated species in solution are kept intact in the gas-phase being detected in the mass spectrum. Therefore, the observed dimer species where two ibuprofen molecules are associated via hydrogen bonding ($[2Ibu - H]^-$) is most likely a result of intermolecular interactions in the solution phase, as was established for other ibuprofen derivatives too.[43] Moreover, this

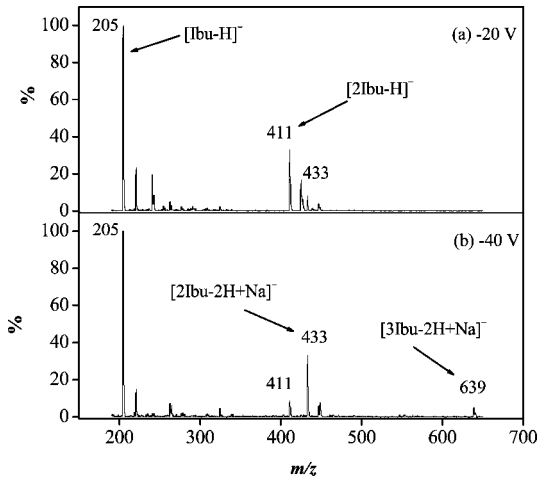

Figure 2. ESI mass spectra, relative intensity (% of spectral intensity with respect to the most intense peak - the deprotonated molecular ion, $[Ibu - H]^-$) vs *m/z* of ibuprofen in methanol solution, obtained in the negative ionization mode with cone voltages of (a) −20 V and (b) −40 V. The peaks of interest are as follows: $[Ibu - H]^-$, $m/z = 205$; $[2Ibu - H]^-$, $m/z = 411$; $[2Ibu - 2H + Na]^-$, $m/z = 433$ and $[3Ibu - 2H + Na]^-$, $m/z = 639$.

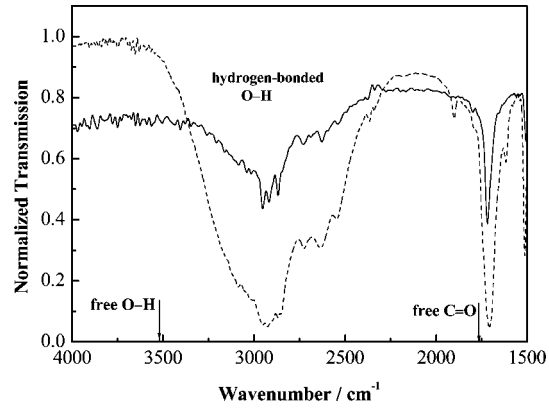

Figure 3. Infrared spectra of crystalline (solid line) and supercooled liquid (dashed line) Ibuprofen at room temperature. The wavenumbers of the free O−H and C═O stretching vibrations are indicated by arrows, the respective absorption intensities are low in both spectra showing that the ibuprofen molecules form almost hydrogen bonding aggregates.

peak detected under the milder conditions of Figure 2a diminishes for an increased cone voltage (Figure 2b). This result supports the hypothesis that dimer ion pairs are already present in the solution phase, rather than been formed by a possible association taking place in the gas-phase. Additionally, two sodium adducts were also found. The formation of pseudo molecular ions between analytes and background metal ions in solution phase is a well-known feature of ESI mass spectra.[45,46] For ibuprofen, besides the sodium bridged dimer ion ($[2Ibu - 2H + Na]^-$) already reported,[43] a trimer sodium adduct was also detected upon increasing cone voltage, which can be regarded as an indication that collisions in gas-phase are responsible for adduct formation due to an increased number of gas-phase collisions. However, the trimer species detected maintains a hydrogen bond between two monomers that could exist previous to sampling. A more detailed discussion is beyond the scope of this work; nevertheless these results confirm the strong tendency of ibuprofen molecules to form noncovalent bonded aggregates. This will be further elucidated by both FTIR measurements and simulation studies.

Infrared Spectroscopy. In order to probe intermolecular interactions as hydrogen bonded (HB) associations between ibuprofen molecules, infrared spectroscopy was used to analyze both crystalline and supercooled (amorphous) ibuprofen at room temperature. The wavenumber regions of particular interest are located around 3000 and 1700 cm^{-1}, due to the absorption bands of O−H and C═O stretching modes, respectively. Free O−H and C═O have characteristic frequencies at approximately 3520 and 1760 cm^{-1} appearing as sharp lines.[47] In the presence of hydrogen bonds these stretching vibrations are perturbed: the C═O band shifts down to lower wavenumbers (1700−1725 cm^{-1}) and the O−H vibration gives rise to a broadband between 3300−2500 cm^{-1} (ref 47). The contribution attributed to the free OH and CO groups is rather small in the spectra presented in Figure 3 (nevertheless the corresponding frequencies are indicated by arrows). The characteristic bands are assigned to hydrogen bonded groups in both crystalline and supercooled ibuprofen. Similar features are reported for FTIR studies involving hydrogen-bond interaction in materials that also contain carboxylic groups.[48,49] Thus it can be concluded that the ibuprofen molecules exist almost in the form of hydrogen bonded aggregates in both phases. The major difference between them is the lower intensity and the broader bands in the spectrum of the supercooled liquid due to its less organized structure.

It is also reported from X-ray diffraction that in racemic crystalline ibuprofen, one *R* and one *S* molecule form a cyclic dimer through a strong double-hydrogen bond involving the COOH acid groups, organized in the monoclinic $P2_1/c$ space group.[37,50] These IR results corroborate the affinity of ibuprofen molecules to form hydrogen bonded aggregates, such as dimers or trimers, as concluded from the ESI-MS results. It should be strongly underlined that the combination of experiments reported here verifies the existence of hydrogen bonded aggregates also in the supercooled state. That will strongly affect the dielectric behavior of ibuprofen, as discussed later.

Molecular Dynamics Simulations. Hydrogen bonding statistics can be obtained from molecular dynamics (MD) simulation and compared to the experimental results. Especially the population of different HB associated structures can be estimated, which is a useful tool to probe the structure of liquid ibuprofen. In the present study, two oxygen atoms are considered to be H-bonded if (i) they do not belong to the same molecule, (ii) the oxygen−oxygen distance is less than 3.4 Å, and (iii) the O−H−O angle is larger than 120°.[51] This criterion allows to include more deformed and weaker HBs in the statistics. Each ibuprofen molecule has two oxygen atoms localized in the carboxylic acid group COOH which can form hydrogen bonds. The carbonyl oxygen site acts as proton acceptor and can only form HB with hydroxyl oxygen sites of other ibuprofen molecules. The hydroxyl oxygen site may act both as acceptor and donor. MD calculations reveal that the fraction of hydroxyl oxygen's forming HBs with other hydroxyl oxygen's is only 0.24 while it is 0.76 with the carbonyl oxygen's. Therefore, cyclic HB associated structures displayed in Figure 4 should be strongly favored.

The fraction of ibuprofen HB hydroxyl oxygen sites forming simultaneously n_s HBs with other neighboring ibuprofen HBs sites either carbonyl or hydroxyl sites is 0.28, 0.63 and 0.09 for $n_s = 0$, 1 and 2 respectively. The number of sites participating in more than $n_s = 2$ HBs is negligible. Results for the HB carbonyl oxygen sites are 0.41, 0.57, and 0.02. This result indicates that the structure of ibuprofen is not dominated by long chains of open double hydrogen bonded molecules corresponding to $n_s = 2$ (see Figure 4c) as usually seen for alcohols.[52] Instead, liquid ibuprofen mainly consists of single

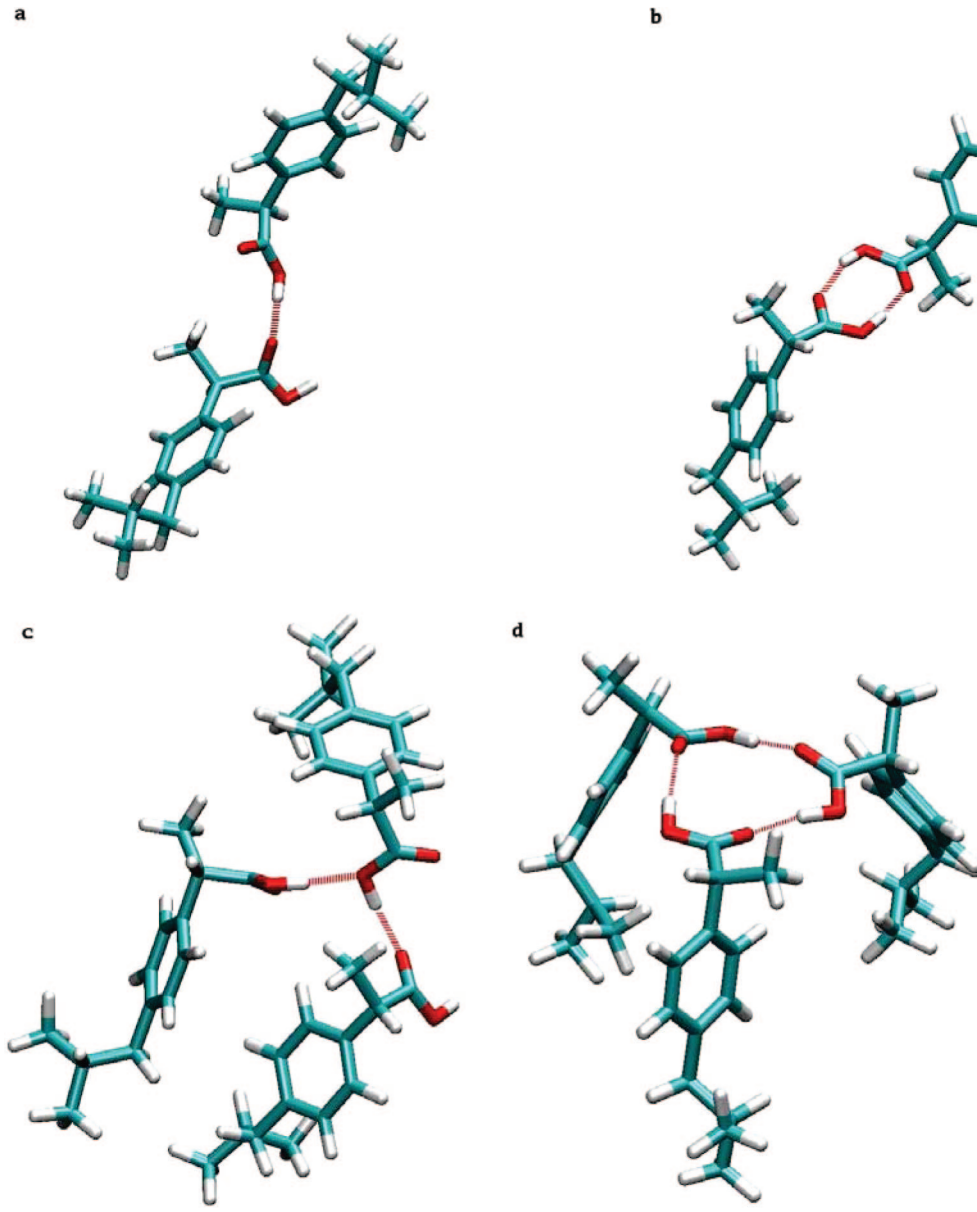

Figure 4. Snapshots of possible hydrogen bonded aggregates of ibuprofen molecules obtained from MD simulations: (a) linear dimer, (b) cyclic dimer, (c) linear trimer, and (d) cyclic trimer.

HB molecules ($n_s = 1$) (Figure 4, parts a, b, and d). Therefore, fundamental differences are likely to exist between ibuprofen and alcohols in their dielectric properties as discussed below. Moreover, the $n_s = 0$ fraction can be compared with the intensity of the bands characteristic for free OH and free C═O observed in the IR spectra. At $T = 360$ K in the simulation, the fraction of non-hydrogen bonded sites is large compared to the IR results shown in Figure 3 for a slightly different temperature of $T =$ 300 K. This spectra point to a low amount of free OH and free CO. However, additional MD simulations performed at higher temperatures indicate a clear decrease of the value of the $n_s =$ 0 fractions with decreasing temperature. Linear extrapolations to $T = 300$ K leads to 0.18 for the fraction of free OH and 0.30 for the fraction of free CO which seems still too high. Most likely, the simulation procedure overestimates the number of nonaggregated ibuprofen molecules. However, it should be underlined that it gives clear-cut evidence for hydrogen bonded aggregates and there structures. For further discussion the dependence of $n_s = 0$ as function of temperature below $T =$ 360 K might be interesting but additional time-consuming calculations are required, which will be discussed elsewhere.

The fraction of multimers composed of n ibuprofen molecules detected on average during the MD simulation is displayed in Figure 5. A large variety of aggregates are theoretical possible as also suggested by the electrospray ionization mass spectroscopy and the broad adsorption peaks in the FTIR spectra.

The fraction of isolated molecules ($n = 1$) is found to be lower than those of dimers ($n = 2$), trimers ($n = 3$), and tetramers ($n = 4$) which are expected to be the most probable structures from the simulations. Additional larger associated structures are also observed but their fraction is small at this temperature. Most important is the contribution of linear and cyclic geometries to the total number of dimers and trimers structures which is summarized in Table 1. Cyclic tetramers are not considered in the following since their fraction is negligible (below 1%) in the MD simulations. Oppositely, Table 1 reveals a significant contribution of cyclic structures to the total number of dimers and trimers (see also Figure 5): 43% and 31% for the dimers and the trimers respectively. This result is consistent with the reported structures of racemic and nonracemic crystalline ibuprofen in which the molecules form hydrogen-bonded cyclic dimers.[37,53,54] Moreover, these cyclic

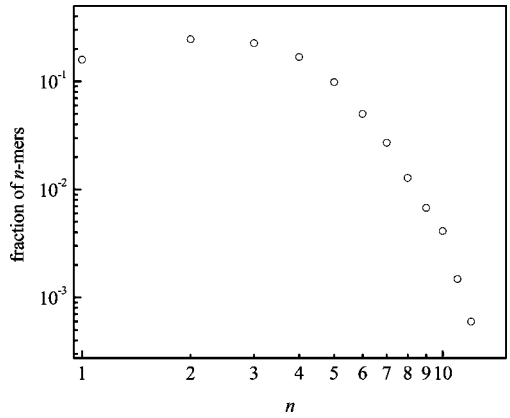

Figure 5. Fraction of ibuprofen intermolecular hydrogen bonded structures (*n*-mers) as function of the number of molecules *n* involved in the different multimers as obtained from MD simulation for $T = 360$ K. See Figure 4 for snapshots of some examples of hydrogen bonded aggregates.

TABLE 1: Fraction, Lifetimes, Average Dipole Moments (μ) and Kirkwood Correlation Factors (g_K) of Cyclic and Linear Geometries of the Dimers and Trimers Structures As Obtained from the MD Simulations

	dimers		trimers	
$T = 360$ K	cyclic	linear	cyclic	linear
fraction %	43	57	31	69
lifetime (ps)	346	33	226	13.6
μ (D)	1.29	2.15	1.68	2.50
g_K	0.32	0.89	0.38	0.83

structures are found to be extremely stable compared to the linear ones. Indeed, the survival probability of the intermolecular HBs structures formed between the different ibuprofen molecules has been estimated from the time decay of the intermittent correlation function $C_n(t) = \langle h_n(t) \cdot h_n(0) \rangle$ where $h_n(t)$ is unity if a given multimer composed of n molecules formed at time 0 remains intact at time t—even if it has broken in between—and is zero otherwise. [52,55] The lifetime of one multimer of size n is defined as the time $C_n(t)$ decays from 1 to $1/e$. Lifetimes of dimers and trimers either cyclic or linear are reported in Table 1. This shows that the estimated lifetimes of cyclic geometries are about one decade longer than that of the linear ones.

3.2. Thermal Transitions Studied by DSC and DRS. To achieve the conditions to obtain ibuprofen in the supercooled and glassy states, differential scanning calorimetry is carried out in three successive scans (Figure 6).

In the first scan, ibuprofen was heated to 353 K. An endothermic peak, with an onset at 347 K, identifies the melting of the sample at the melting temperature T_m which is typical for the racemic mixture.[30,31] The enthalpy of fusion is 25.5 kJ·mol^{-1} in agreement with the value reported by Xu et al..[56] In the subsequent cooling scan (run 2) crystallization is avoided, there is no exothermic peak close to T_m. Continuous cooling leads to the glass transition around 228 K. The subsequent heating scan, run 3, from the glassy state, shows the characteristic signature for the glass transition in the heat flow with an onset at $T_g = 228$ K, along with an enthalpy overshoot. The heat capacity step at the glass transition is $\Delta C_p = 0.37$ J·K^{-1}·g^{-1} = 76 J·K^{-1}·mol^{-1}. The sample does not recrystallize during heating to 353 K. These results are in good agreement with those reported by Dudognon et al.[57]

The melting of ibuprofen was also monitored by DRS by measuring $\varepsilon^*(\omega)$ from room temperature up to 353 K with a heating rate of 1 K/min, using a compressed disk sample;

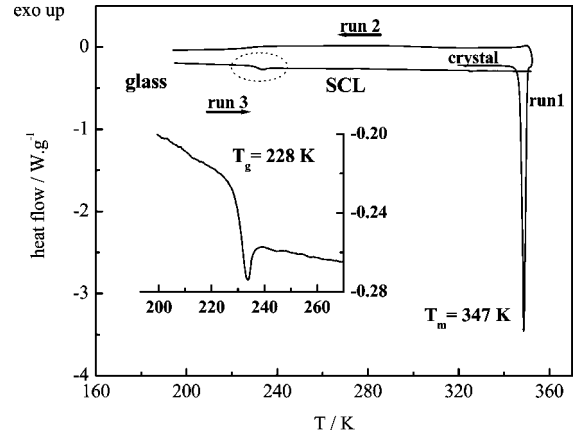

Figure 6. DSC thermograms of ibuprofen obtained during heating/cooling with 5 K/min. Run 1: Heating of the as received crystal; $T_m = 347$ K is the extrapolated onset melting temperature. Run 2: Subsequent cooling of the melt from 353 K down to 193 K. Run 3: Following heating of the vitrified ibuprofen to a temperature higher than T_m. The inset enlarges the glass transition region obtained on heating. $T_g = 228$ K is the onset glass transition temperature; at higher temperatures there is no evidence of recrystallization.

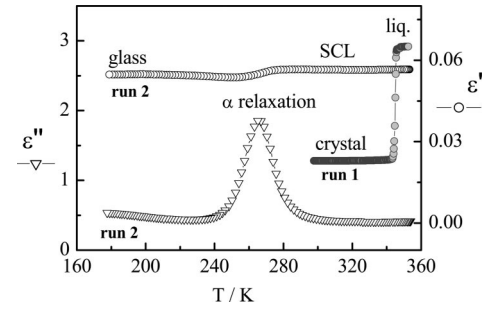

Figure 7. Temperature dependence of the real, ε' (circles) and imaginary, ε'' (triangles) part of the complex dielectric function for a frequency $f = 10^5$ Hz. Run 1: DRS result obtained on heating at 1 K/min of a compressed disk of the as received crystalline ibuprofen. The observed step increase of ε' (gray filled circles) is the melting transition, however can not be taken quantitatively since thickness changes occurred. Run 2: DRS result recorded on cooling with 10 K/min, after annealing at 353 K for 1 h, evidencing the bypass of crystallization and further occurrence of glass transition. The ε' scale is only valid for run 2 (see text for details).

measurements using a powder sample (without compressing) give highly scattering data approaching the melting temperature. The real part of the complex permittivity, ε', at a frequency of 10^5 Hz, is plotted in Figure 7, versus temperature (run 1). ε' shows a steep increase with a midpoint at 345 K (gray filled circles) in good agreement with calorimetric measurements. Absolute values for ε' are omitted due to the fact that both thickness and volume of the sample changes during melting.

During subsequent cooling with a rate of 10 K/min (run 2), after the sample being kept at 353 K, no discontinuity occurs around T_m, indicating that crystallization does not take place and a supercooled liquid is obtained (SCL in Figure 7). ε' (open circles) remains constant down to 273 K followed by a step indicating the dynamic glass transition (α-relaxation) accompanied by the corresponding dielectric loss peak in ε'' (triangles).

It must be emphasized that ε' is a useful property to probe melting and crystallization transitions, with the advantage of being frequency independent and not being affected neither by conductivity nor implying any data modeling. Thus, ε' has a practical importance to monitor phase transitions in pharmaceutical compounds.

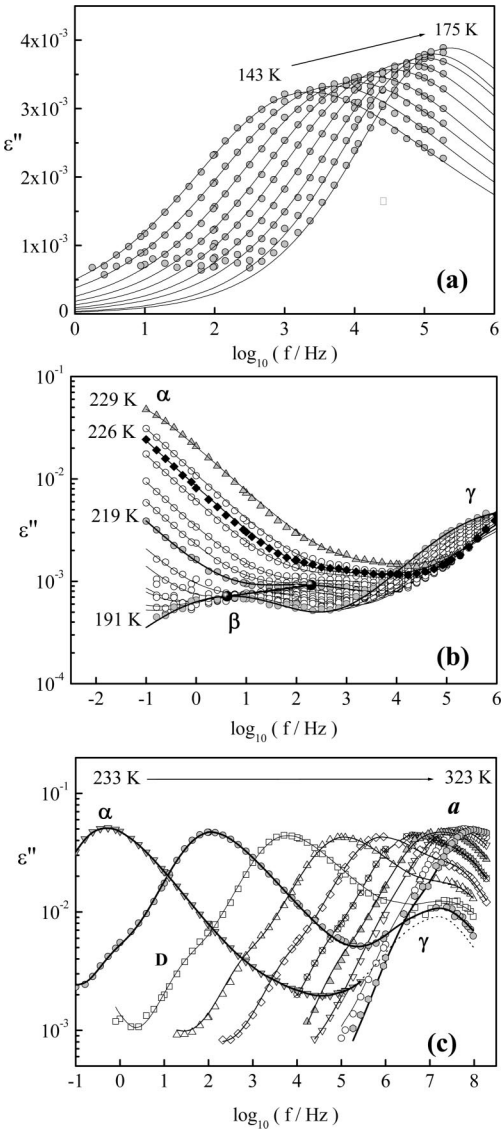

Figure 8. (a) Dielectric loss versus frequency in the glassy state, in steps of 4 K from $T = 143$ K to $T = 175$ K. (b) Dielectric loss versus frequency from 191 K to $T = 229$ K in steps of 2 K. Filled black circles correspond to the detected β-process in the glassy state, whose relaxation rate follows an Arrhenius temperature dependence (Table 2). Filled diamonds represent the isothermal data taken at 226 K which corresponds to $T_g^{diel}(\tau = 100$ s). (c) Dielectric loss spectra above the glass transition temperature between 233 and 323 K, in steps of 10 K. For clarity reasons, at temperatures higher than 243 K, when the conductivity contribution becomes important, data and fitting curves have been suppressed from the lower frequency part of the spectra. In parts a−c, the solid lines are the overall HN fitting curves to data.

3.3. Dielectric Characterization of the Molecular Mobility of Ibuprofen. The ε' trace at 10^5 Hz obtained under isothermal conditions is similar to that of Figure 7. The experimental procedure is equivalent to effective cooling rates less than 1 K/min (~ 0.6 K/min in the temperature range from 353 to 273 K and ~0.2 K/min from 273 to 143 K). Under this condition, ibuprofen easily supercools with no need of high cooling rates. However, crystallization can occur during the cooling when the time spent previously in the molten state is too short to eliminate all crystallization nuclei. Therefore the sample is kept for 1 h in the molten state at $T = 353$ K prior to the measurement. Moreover, it was also observed that if the supercooled liquid is stored at room temperature for several hours, or even days, without any external perturbation, crystallization does not occur.

Parts a−c of Figure 8 show illustrative dielectric loss spectra acquired in the available frequency range covering a wide temperature interval from the glass to the supercooled state. Multiple relaxation processes take place in ibuprofen. In the glassy state at the lowest temperatures, a well defined broad secondary process with a weak intensity is observed, here designated as γ (Figure 8a). At temperatures between 191 and 229 K, another secondary relaxation process, with even lower intensity moves inside the frequency window with increasing temperature, labeled as β (Figure 8b). In the supercooled state this process becomes submerged under the main relaxation process (α-relaxation) associated with the dynamic glass transition (Figure 8c). In the mega to gigahertz frequency region it is possible to observe the high frequency part of the α-process and the secondary γ-relaxation that shifts out from the low frequency window. At higher temperatures, the intensity of the secondary γ-process becomes comparable to the magnitude of the main α-process and both merge to a single process (for $T > 311$ K), here named *a* (Figure 8c). Moreover, at temperatures higher or frequencies lower than for the α-process (Figure 8c), a less intense process named D is observed which persists active in the whole studied temperature range, even for temperatures higher than the overlapping of the α- and γ- processes.

Equation 1 was fitted to the isothermal dielectric data where additive behavior is assumed. Figure 9 gives three representative examples for this procedure where both the real and the imaginary parts were used in the fits.

This fitting procedure allows us to extract the spectral shape, the dielectric strength, and the relaxation time for each process which are discussed in the following in detail.

(i) Spectral Shape. Both secondary relaxation processes show a non Debye behavior. The peak of the γ-relaxation (for $T < T_g$) is broad ($\alpha_{HN} \sim 0.5$) and asymmetric ($\alpha_{HN}{}^*\beta_{HN} = 0.2$); above T_g, for temperatures higher than 233 K, the shape parameters of the γ-relaxation change significantly ($\beta_{HN} = 1$ and $\alpha_{HN} \sim 0.6-0.8$).

The β-process, in the subglass temperature region, can be well described by a symmetrical Cole−Cole function (*i.e.*, $\beta_{HN} = 1$) with $\alpha_{HN} \sim 0.45$; these parameters were kept constant in the narrow temperature range above T_g where it was still possible to follow the β-trace.

The shape of the α-relaxation has a weak temperature dependence ($\alpha_{HN,\alpha} \approx 0.81$; $\beta_{HN,\alpha} \approx 0.52$), allowing to construct a master curve. Figure 10 presents the reduced plots of $\varepsilon''/\varepsilon''_{max}$, where ε''_{max} is the maximum loss of the α-peak, against $\log(f/f_{max})$, obtained between 232 and 262 K. The D-process that shows up in the low frequency flank is characterized by a Debye-like behavior ($\alpha_{HN} = 1$; $\beta_{HN} = 1$). To describe the data

TABLE 2: Estimated Parameters of the Arrhenius Fit, $\tau(T) = \tau_\infty \exp(E_a/RT)$, to the Secondary γ- and β- Relaxation Times, and of the VFTH Fit, $\tau(T) = \tau_\infty \exp(B/(T - T_0))$, to the α, *a* and D-Relaxation Times

γ-process ($T < T_g$)		β-process ($T < T_g$)		α, *a* processes				D-process		
E_a/kJ·mol^{-1}	τ_∞/s	E_a/kJ·mol^{-1}	τ_∞/s		B/K	τ_∞/s	T_0/K	B/K	τ_∞/s	T_0/K
30.5 ± 0.7	$(6 \pm 4) \times 10^{-16}$	52 ± 2	$(3 \pm 4) \times 10^{-16}$	**VFTH$_1$**	1426 ± 50	$(1.2 \pm 0.6) \times 10^{-14}$	187 ± 1	1379 ± 49	$(0.9 \pm 0.3) \times 10^{-12}$	191 ± 1
				VFTH$_2$	792 ± 13	$(1.7 \pm 0.1) \times 10^{-12}$	205.6 ± 0.6			

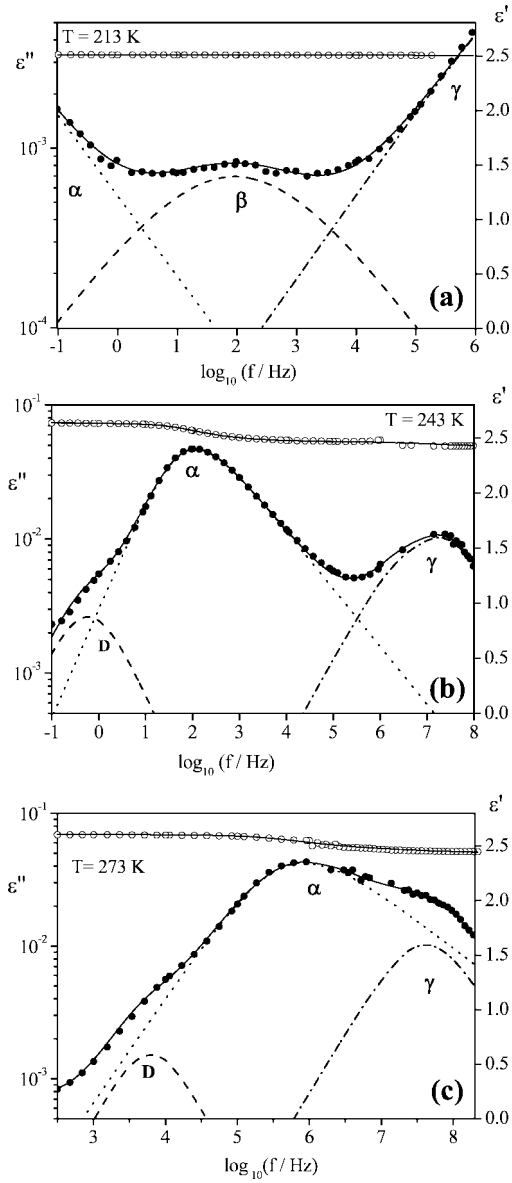

Figure 9. Three examples of the fitting procedure where an additive contribution of three HN-functions is assumed: both the real (open circles) and the imaginary (filled circles) part of complex permittivity were included at (a) 213 K, (b) 243 K, and (c) 273 K. The solid lines represent the overall fit and the dashed lines the individual HN-functions (Cole−Cole for the β-process, HN for γ- and α- relaxations and, Debye function for the D-process; for details see section "*Spectral Shape*" in the main text).

for $T > 262$ K, where the experimental frequency range was extended up to 10^9 Hz, the shape parameters of the main relaxation were constrained to vary within the range of values found for lower temperatures ($\alpha_{HN,\alpha} = 0.81 \pm 0.02$; $\beta_{HN,\alpha} = 0.54 \pm 0.02$). For the D-process the Debye character is still assumed in accordance with the experimental data.

The non-Debye nature of the relaxation response in supercooled liquids can also be described in the time domain, by the well-known Kohlrausch−Williams−Watts (KWW) function:[58,59]

$$\varphi(t) = \exp\left[-\left(\frac{t}{\tau_{KWW}}\right)^{\beta_{KWW}}\right] \quad (3)$$

where τ_{KWW} is a characteristic relaxation time and β_{KWW} is the so-called "stretching parameter" ($0 < \beta_{KWW} \leq 1$; $\beta_{KWW} = 1$ for a Debye response). Fitting the normalized HN function that describes the α-loss peak (solid line in Figure 10) by the one-side Fourier transformation of the stretched exponential function, a β_{KWW} value of 0.52 is obtained (dashed line in Figure 10). This value matches the value estimated from the empirical correlation proposed by Alegria et al.[60] and is similar to the value reported by Johari et al. ($\beta_{KWW} = 0.54$).[2] The estimated KWW parameters will be later used for a quantitative discussion.

(ii) Dielectric Strength. The temperature dependence of the dielectric strength, $\Delta\varepsilon$, for the different processes is shown in Figure 11.

Considering the polar carboxylic moiety (see structure in Scheme 1) and the dipole moment of 1.64 Debye as found by MD simulations for an isolated molecule, the estimated dielectric strength is rather low, even for the α-process. The starting point for the analysis of $\Delta\varepsilon$ is the extension of the Debye theory by Onsager, Fröhlich, and Kirkwood (see ref 61 and references therein).

$$\Delta\varepsilon = \frac{1}{3\varepsilon_0} g_K F \frac{\mu_0^2}{k_B T} \frac{N}{V} \quad (4)$$

ε_0 is the vacuum permittivity, μ_0 the dipole moment of the moving unit in vacuum, $F \approx 1$ is the Onsager factor calculated in the frame of the reaction field, T the temperature, k_B the Boltzmann constant, N/V the number density of dipoles. g_K is the Kirkwood correlation factor to take into account short-range intermolecular interactions that lead to specific static dipole−dipole orientations. For predominantly parallel or antiparallel correlations between neighboring dipoles, $g_K > 1$ or $0 < g_K < 1$, respectively, while for a random orientation of dipoles $g_K = 1$ holds. The small values of $\Delta\varepsilon$ agree with that of Johari et al.,[2] which conclude that hydrogen-bonding in ibuprofen favors an antiparallel correlation of the dipole vectors. In order to get an insight in the origin of the low dielectric strength from the molecular point of view, average dipole moments and Kirkwood correlation factors for cyclic and linear geometries of the dimers and trimers structures were calculated from the MD simulations. The corresponding values are summarized in Table 1. The calculated Kirkwood factors $g_K < 1$ verify the antiparallel correlation of the dipoles. This is specifically true for cyclic dimers and trimers which are present in larger fractions (see Table 1). Moreover the dipole moments are found to be smaller for the cyclic aggregates than for the linear ones. Both results

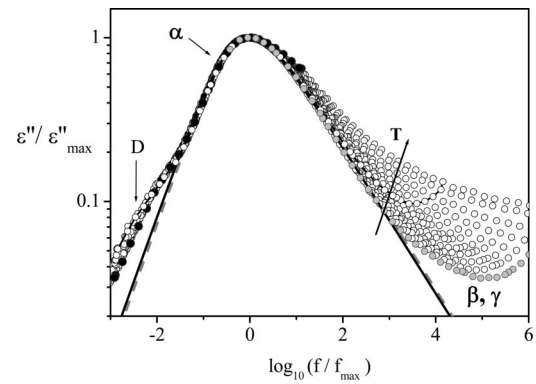

Figure 10. Dielectric loss curves in the frequency domain $10^{-1}-10^6$ Hz, normalized for the α-relaxation for temperatures between 232 K (gray filled circles) and 262 K (black filled circles) illustrating its invariant shape. The high frequency side is affected by the secondary processes. The solid line represents the individual HN function used to fit the α-process with $\alpha_{HN} = 0.81$ and $\beta_{HN} = 0.56$. The dashed line is the corresponding fit of the one-sided Fourier transform of the KWW function with $\beta_{KWW} = 0.52$.

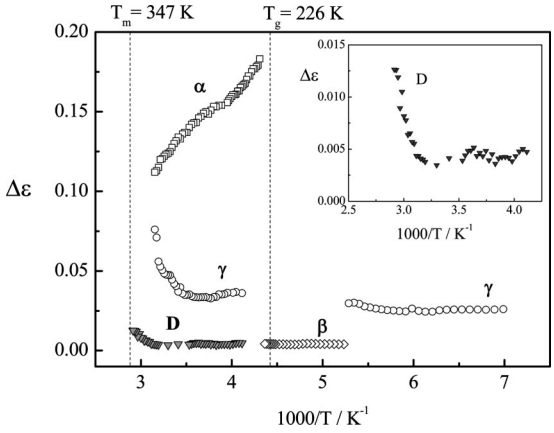

Figure 11. Dielectric strength, $\Delta\varepsilon$, for the α, β, γ, and D process versus 1/T. The inset enlarges $\Delta\varepsilon$ vs 1/T plot for the D-process.

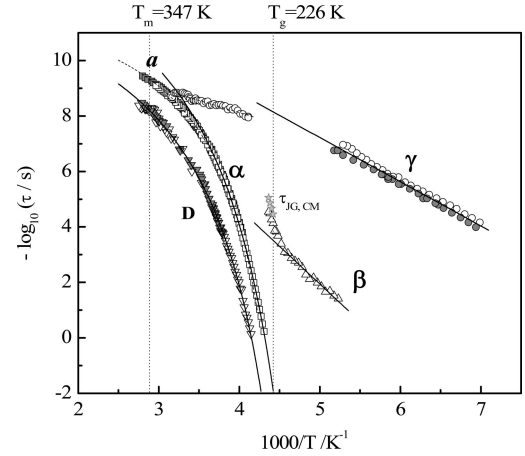

Figure 12. Relaxation time, τ, versus 1/T for all processes: open symbols, isothermal loss data collected during cooling; gray filled symbols, τ obtained from the isochronal plots for all studied frequencies f ($\tau = 1/(2\pi f)$, $1/T_{max}$). The γ-process runs out from the low-frequency window at ~193 K becoming again detectable in the high frequency range where measurements were only performed for temperatures above 243 K (reason for the gap of data close to T_g). Lines are fits of the Arrhenius and VFTH formulas to the corresponding data: in the α,*a* trace the solid line is the $VFTH_1$ fit and the dashed line is the $VFTH_2$ fit to the data (see text and parameters in Table 2). Light gray stars indicate the JG relaxation time, $\tau_{JG,}$ estimated from Coupling Model (eq. 5). Vertical dashed lines are the dielectric glass transition temperature $T_g^{diel.}$ (τ = 100 s) = 226 K and the melting temperature T_m = 347 K.

are consistent with the low measured dielectric strength. Furthermore, it should be mentioned that the average dipole moment of the cyclic dimers is even smaller than that of the isolated molecule (1.64 D). This result is consistent with the estimation of a weak dipole moment from the *ab initio* calculations[40] of the isolated racemic (0.00 D) and nonracemic (0.54 D) cyclic dimers as found in crystalline ibuprofen.[37,53,54] However, the values of the dipole moment of the cyclic dimers obtained in the disordered phase (50:50 mixture of racemic/nonracemic) are significantly higher than that for crystalline one since the structures might have distorted geometries.

Concerning the temperature dependence of the dielectric strength, the intensity of both β- and γ- relaxations are almost temperature independent in the glassy state. However, the intensity of the γ-process increases strongly in the temperature range close to the merging with the α-relaxation (see Figure 11). The same behavior was observed in other systems.[62−65] For an epoxy resin it was argued that local motions couple with diffusive motions dominating at temperatures above T_g.[66] This could be the case for ibuprofen, where the local motions that originate the γ-relaxation are probably molecular fluctuations of carboxylic groups.

For the α-process, the $\Delta\varepsilon$ decreases with increasing temperature as it is well know for conventional glass formers and polymers. It should be noted that the corresponding temperature dependencies are much stronger than predicted by eq 4, which will be explored with more detail later in the text.

In regard to the Debye process, at the lowest temperatures its dielectric strength is almost temperature independent, while at temperatures above ~313 K, $\Delta\varepsilon_D$ increases with increasing temperature (see inset of Figure 11). This behavior will be also discussed later.

(iii) Relaxation Map. Figure 12 shows the temperature dependence of the relaxation time τ for all relaxation processes. Additionally the corresponding values of τ obtained from the isochronal plots ($\tau = 1/(2\pi f)$, $1/T_{max}$) are given. The two data sets coincide well. The agreement between the two methods validates the use of isochronal data especially when the respective loss peaks maxima are poorly defined in the frequency domain or out of the accessible frequency range. This method has also been proved to be advantageous in distinguishing multiple processes.[34,67,68]

Due to the multiple relaxation processes found in ibuprofen, for the sake of clarity the relaxation map will be analyzed in order of increasing temperature.

γ- and β-Process. In the glassy state the relaxation time for the two secondary processes (γ and β) follow a linear temperature dependence of log(τ) versus 1/T as expected for relaxation processes related to localized molecular mobility. From the Arrhenius equation $\tau(T) = \tau_\infty \exp(E_a/RT)$ (R = ideal gas constant), values of the activation energy E_a of 31 and 52 kJ·mol^{-1} were estimated for the γ- and the β-relaxation respectively (see Table 2) for temperatures below T_g. For the γ-process the two sets of data, isothermal and isochronal, were included in the analysis. Above T_g, the temperature dependence of the relaxation time of the γ-process bents toward that of the α-process; the corresponding apparent activation energy is lower than that found in the glassy state. A similar behavior is reported for dialkyl phthalates[69] and glass forming epoxy resins where, in the later the authors emphasize that it is not a fitting artifact since the two processes are, at least, two decades apart allowing a properly spectral deconvolution.[70] Also for ibuprofen, the α- and the γ-process are well separated in this temperature range by several decades (see Figure 8c). As suggested by a reviewer, the observed slowing down of the γ-relaxation, which is a general behavior, is due to its hybridization with the β-relaxation when the two relaxations times get close to each other.

The temperature dependence of the relaxation time of the β-process shows also a strong change around T_g; *i.e.*, the Arrhenius-like temperature dependence of τ_β below T_g cannot be extrapolated to temperatures above T_g. This crossover of the τ_β trace below the glass transition to stronger temperature dependence above T_g has been observed directly in the raw data for different systems.[71−73] This behavior can be discussed in the framework of the coupling model (CM).[74] It postulates a so-called primitive relaxation process as a precursor of the α-relaxation which is the analogue of the "genuine"[75] Johari−Goldstein (JG) process.[76] The CM predicts a correlation of the relaxation time of the JG-process, τ_{JG}, with that of the α-process which reads:

$$\tau_{JG}(T) \approx \tau_0(T) = t_c^{\,n}[\tau_\alpha(T)]^{1-n} \quad (5)$$

τ_0 is the primitive relaxation time of the CM, the coupling parameter $n = 1\text{-}\beta_{KWW}$, τ_α is the relaxation time of the KWW function (τ_{KWW} in eq 3) and t_c is a time characterizing the crossover from independent to cooperative fluctuations found to be close to 2×10^{-12} s for molecular glass-formers.[63] Using $\beta_{KWW} = 0.52$, eq 5 gives a value of τ_{JG} at T_g of 4×10^{-5} s in good agreement with the experimental τ_β value at this temperature (see Figure 12). Also for higher temperatures a good agreement with τ_β is observed. This shows that the changed temperature dependence of τ_β above T_g is consistent with the CM[71] and indicates that the β-process of ibuprofen is a "genuine" Johari−Goldstein relaxation. Furthermore, below T_g the activation energy of the β-process estimated from the Arrhenius equation (see Table 2) gives for the ratio E_a/RT_g a value of 28 in accordance with values found for that ratio obtained for genuine JG relaxation processes observed for several glass formers[77] (this is slightly higher than the value of 24 as proposed by Kudlik et al.,[78] $E_{a,JG} = 24RT_g$). Additionally, the Cole−Cole type of the detected β-process is consistent with the usually found profile of the Johari-Goldstein β-relaxation.[79] All these features points to the direction that the detected β-relaxation is a Johari-Goldstein process as also found in other conventional and pharmaceutical glass formers such as sorbitol,[80] indomethacin,[19] and aspirin.[20,81]

A different way to rationalize the change in activation energy of the β-process at T_g is to assume that the actual relaxation rate is free volume dependent.[82] Since the free volume significantly increases upon passing the glass transition this will accelerates the relaxation rate that results in a corresponding increase in the apparent activation energy.

The α- and a-Relaxation. For the α-relaxation the temperature dependence of the relaxation time is curved when plotted versus $1/T$ (see Figure 12). Close to T_g, this dependency is often described by the empirical Vogel−Fulcher−Tammann−Hesse (VFTH) equation[83−85]

$$\tau(T) = \tau_\infty \exp\left(\frac{B}{T - T_0}\right) \quad (6)$$

where τ_∞ and B are parameters and T_0 is the so-called Vogel temperature found to be 50 to 70 K below T_g. For conventional glass formers and polymers it is known that a single VFTH-law describes the temperature dependence of the relaxation times only up to a temperature $T_B \approx (1.2 - 1.3)\ T_g$. At T_B, the temperature dependence of τ_α changes from a low temperature VFTH behavior to a high temperature one.[86,87] For a detailed analysis of the temperature dependency of the α-relaxation of ibuprofen a derivative method is applied.[70,87−89] This method, is sensitive to the functional form of τ(T) irrespective of the pre-exponential factor. For a dependency according to the VFTH equation (eq 6) one gets

$$\left[\frac{d(\log_{10}(1/\tau))}{dT}\right]^{-1/2} = \left(\frac{B}{\ln 10}\right)^{-1/2}(T - T_0) \quad (7)$$

Thus, in a plot of $[-d(\log_{10}(\tau))/dT]^{-1/2}$ versus temperature, a VFTH behavior shows up as a straight line. In the following this type of analysis is applied to the dynamic glass transition. Figure 13a shows that for ibuprofen at least two VFTH equations (one at high $VFTH_2$ and one at low temperatures $VFTH_1$) have to be used to describe the data in the whole temperature range. This is shown for ibuprofen for the first time.

The derivative analysis shows that $VFTH_1$ and $VFTH_2$ have distinct Vogel temperatures that differ about 20 K, with $T_{0,1} < T_{0,2}$ indicating a different dynamical behavior in the low and high temperature regime. The intersection of the two VFTH lines gives a crossover temperature $T_B = 265$ K. These fits are shown respectively as solid ($VFTH_1$) and dashed ($VFTH_2$) lines in the relaxation map (Figure 12) and the characteristics parameters are presented in Table 2.

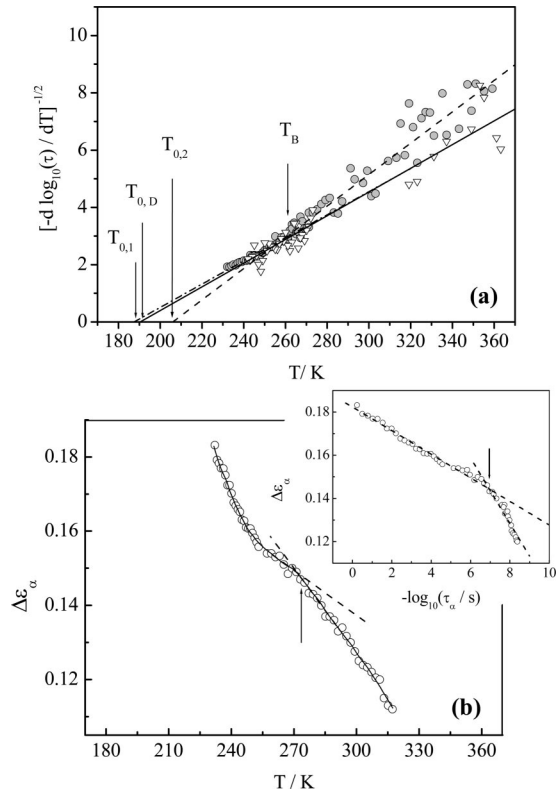

Figure 13. (a) $[-d(\log_{10}(\tau))/dT]^{-1/2}$ vs temperature for the relaxation time of the α, *a* (circles) and the Debye (triangles) processes. The dash-dotted line is a linear regression to the low-temperature α-relaxation data where $VFTH_1$ regime holds with a Vogel temperature $T_{0,1}$, while the dashed line is the linear fit to the high temperature data characterized by $VFTH_2$ with $T_{0,2}$. The intersection of the two lines defines the crossover temperature $T_B = 265$ K. The solid line is the linear fit to the Debye data characterized by a VFTH law with $T_{0,D}$. (b) Temperature dependence of the α-relaxation dielectric strength, $\Delta\varepsilon_\alpha$. Lines are guides for the eyes. The arrow indicates a crossover temperature separating the high and low temperature region in agreement with the T_B value calculated from the intersection of the $VFTH_1$ and $VFTH_2$ law. The inset gives $\Delta\varepsilon_\alpha$ versus $-\log_{10}(\tau_\alpha)$. The intersection of the two temperatures regimes is indicated by the arrow which gives a relaxation time corresponding to the crossover temperature of the $\Delta\varepsilon_\alpha$ vs temperature plot.

The existence of a crossover in the temperature dependence of the α-relaxation can be revealed also by its dielectric relaxation strength, which is replotted as a function of temperature in Figure 13b. Besides its strong increase with decreasing temperature (see also Figure 11), two well separated regions are observed which can be approximated by two different dependences of $\Delta\varepsilon_\alpha$ versus temperature. The change from the low temperature behavior to the high temperature dependence takes place close to T_B, in a similar way as occurring for other glass formers.[90] Having in mind that the crossover phenomenon was estimated from two different properties, the static quantity dielectric strength and the dynamic relaxation time, a correlation between both is expected as emphasized in ref 87. The plot of $\Delta\varepsilon_\alpha$ versus $\log_{10}(1/\tau_\alpha)$, shown in the inset of Figure 13b, illustrates the predicted correlation where two regions with different dependencies are observed. Their intersection defines

a model-free crossover time corresponding to the temperature T_B that in the framework of cooperativity models of the dynamic glass transition can be regarded as the onset of cooperative fluctuations.[86,87]

A similar behavior is discussed for several other glass formers.[89−93]

Additionally, the curvature of the $\log_{10}(\tau_\alpha)$ vs $1/T$ plot, i.e., the degree of deviation from Arrhenius-type temperature dependence near T_g, allows one to quantitative measure the fragility as the steepness index m according the following equation:

$$m = \frac{\mathrm{d}(\log_{10}\tau(T))}{\mathrm{d}(T_g/T)}_{T=T_g} \quad (8)$$

Fragility values typically range between $m = 16$ for strong systems and $m \sim 200$ (ref 94) for fragile systems where a marked deviation from an Arrhenius dependence occurs induced by cooperative molecular fluctuations.

Using the VFTH expression and eq 8, m can be calculated according to

$$m = \frac{BT_g}{\ln 10(T_g - T_0)^2} \quad (9)$$

Taking the B and T_0 values of the $VFTH_1$ fit to the α-relaxation (Table 2), a fragility index of $m = 93$ is estimated for ibuprofen, allowing one to classify it as a fragile glass former.[94]

The Debye Type Relaxation. The D-relaxation has similar features to the process found in many hydrogen-bonding liquids reported as Debye-like, observed at lower frequencies than the α-process and lacking a calorimetric signature (see ref 28 and references therein). The reported studies concern mainly alcohols, where this process is the most prominent. In those cases, its dielectric strength exceeds the value expected on the basis of the molecular dipole moments.[28,95] For ibuprofen, the D-process has a rather low dielectric strength, the most intense dielectric process being the α-relaxation. An assignment to specific molecular motions in this class of liquids can not be made unambiguously but correlated dipole orientations through hydrogen bonding are discussed to be in its origin.

From the MD simulations, it is concluded that the cyclic structures are characterized by longer lifetimes and smaller dipole moments and Kirkwood correlation factors (see Table 1). This might imply that the hydrogen bonded cyclic structures may be associated with this Debye peak. In fact, the increase of the dielectric strength with temperature observed for the D-process (inset of Figure 11), can be explained by an increase of g_K and consequently of the effective dipole moment with increasing temperature, which is expected since the antiparallel alignment of the cyclic aggregates will be increasingly less favorable causing an increase of the effective dipole moment. Additional MD simulations are needed in order to validate this conjecture.

Moreover, the hydrogen bonded aggregates can form liquid crystalline mesophases due to a supramolecular arrangement induced by hydrogen bonding interactions[96] that persists in the supercooled state. For example, some of *p*-alkoxybenzoic acids[97] exhibit liquid crystalline properties attributed to their ability to form hydrogen-bonded dimers. The same tendency is observed in salicylsalicylic acid where it is proposed that dimers act as mesogenic units, being in the origin of a nematic phase.[98] Since ibuprofen molecules exist as hydrogen bonded aggregates it is reasonable to assume that specific arrangements of aggregates can give rise to the formation of mesophases. This point needs also further investigation.

Figure 12 shows that the temperature dependence of the relaxation times for the D-process is curved when plotted versus 1/T. The derivative analysis was also applied to this set of data (Figure 13a). A straight line is obtained which proves that the relaxation times of the D-process follow the VFTH equation. The value of the obtained Vogel temperature of 191 K by the derivative plot is similar to that of the low temperature regime of the α-relaxation. Therefore it is concluded that some correlation seems to exist between both processes. Besides the agreement in the low temperature limit revealed by comparable Vogel temperatures, also a convergence is found in the relaxation time at infinite temperature as seen by the resemblance of τ_∞ of $VFTH_D$ and $VFTH_2$ (see Table 2). Assuming that the D-process is associated with hydrogen bonding, the similarity of its temperature dependence with that of the main relaxation could be an indication that the dynamics of the former is governed by the dynamics of the α-relaxation.

4. Conclusions

The crystallization of ibuprofen—which is used in pharmaceutical applications—can be easily avoided. Therefore amorphous ibuprofen, which may have advantageous pharmaceutical properties, is studied from the melt down to the glassy state by a combination of different experimental techniques and molecular simulations.

The existence of intermolecular hydrogen bonded associations was verified in the supercooled liquid by IR spectroscopy, Electrospray ionization mass spectrometry and MD simulations. From the molecular point of view especially ESI and the MD simulations reveal the strong tendency of ibuprofen to form noncovalent molecular aggregates such as dimers and trimers either cyclic or linear. The hydrogen bonded cyclic structures were found to have the longer lifetime, smaller dipole moment and smaller Kirkwood correlation factor.

An almost complete dielectric characterization of ibuprofen in the glassy, supercooled and molten states is provided covering a broad frequency range. The results show that ibuprofen has a complex relaxation map including two secondary relaxations, γ and β, a main α-process associated with the dynamic glass transition and a Debye-like process (D-relaxation).

In the glassy state, the relaxation times of the two secondary relaxation processes have an Arrhenius temperature dependence that changes at T_g. The γ-process located at the highest frequencies probably originates from fluctuations of the carboxylic group. A decrease of its apparent activation energy is observed at temperatures above T_g where its dielectric strength gains in intensity, merging with the dynamic glass transition at even higher temperatures.

The β-relaxation is interpreted as "genuine" Johari−Goldstein (JG) process which is a fundamental characteristic of glass formation. Its apparent activation energy changes at T_g to higher values which can be described by the coupling model.

The temperature dependence of the relaxation time of the α-process is curved in a plot versus $1/T$. A more detailed analysis of this dependence by a derivative technique shows that the α-relaxation has a low and a high temperature branch separated by a crossover temperature $T_B = 265$ K. In both ranges the temperature dependence of the relaxation times τ_α follows the Vogel−Fulcher−Tammann−Hesse formula. The crossover pattern is also reflected in the temperature dependence of the

dielectric strength $\Delta\varepsilon_\alpha$. This is more pronounced in a plot of $\Delta\varepsilon_\alpha$ versus $\log(1/\tau_\alpha)$ which shows sharp defined crossover behavior. Thus two dynamical different regions of the α-relaxation can be distinguished nonambiguously. A steepness or fragility index *m* of 93 was estimated which shows that ibuprofen is a fragile glass former.

At lower frequencies than the α-process an additional relaxation process is observed with a weak intensity compared to the dynamical glass transition. It has similar peculiarities to the Debye process found in a large class of hydrogen bonded liquids like alcohols. The temperature dependence of its relaxation time follows a VFTH law, with a Vogel temperature close to the value found for the low temperature branch of the α-relaxation. This indicates a correlation between both processes.

From MD simulations, it is concluded that hydrogen-bonded cyclic structures might be associated with this D-process. This hypothesis is supported by the temperature dependence of the dielectric strength. The similarity of the temperature dependence of relaxation times of the D-process with that of the main relaxation is an indication that the dynamics of the hydrogen bond dynamics is governed by the dynamic glass transition.

Acknowledgment. The authors thank Professor Dr. J. J. Moura Ramos and Dr. Hermínio Diogo for the facilities in using the calorimetric equipment. N.T.C. and A.R.B. thank the Federal Institute of Materials Research and Testing (BAM) for using its research facilities. Financial support to Fundação para a Ciência e Tecnologia (FCT, Portugal) through Project PTDC/CTM/64288/2006 and the PESSOA partnership Hubert Curien (Proc° 4.1.1) is acknowledged. A.R.B. acknowledges FCT for a Ph.D. grant SFRH/BD/23829/2005. F.A. acknowledges the use of the facilities of the IDRIS (Orsay, France) and the CRI (Villeneuve d'Ascq, France) where calculations were carried out. Financial support by the INTERREG (FEDER) program (Nord-Pas de Calais/Kent) is also acknowledged.

References and Notes

(1) Goodman, L. S.; Gilman, A. *The Pharmacological Bases of Therapeutics*, 8th ed.; Pergamon Press: New York, 1990.
(2) Johari, G. P.; Kim, S.; Shanker, R. M. *J. Pharm. Sci.* **2007**, *96*, 1159.
(3) Debenedetti, P. G.; Stillinger, F. H. *Nature* **2001**, *410*, 259.
(4) Debenedetti, P. G. *Metastable Liquids: Concepts and Principles*; Princeton University Press: Princeton, NJ, 1997.
(5) Angell, C. A. *Science* **1995**, *267*, 1924.
(6) Donth, E.; Huth, H.; Beiner, M. J. *J. Phys.: Condens. Matter* **2001**, *13*, L451.
(7) Yu, L. *Adv. Drug Delivery Rev.* **2001**, *48*, 27, and references therein.
(8) Craig, D. Q. M.; Royal, P. G.; Kett, V. L.; Hopton, M. L *Int. J. Pharm.* **1999**, *179*, 179.
(9) Hancock, B. C.; Zografi, G. *J. Pharm. Sci.* **1997**, *86*, 1.
(10) Andronis, V.; Zografi, G. *Pharm. Res.* **1998**, *15*, 835.
(11) Shalaev, E.; Shalaeva, M.; Zografi, G. *J. Pharm. Sci.* **2001**, *91*, 584.
(12) Hancock, B. C.; Shamblin, S. L.; Zografi, G. *Pharm. Res.* **1995**, *12*, 799.
(13) Yoshioka, M.; Hancock, B. C.; Zografi, G. *J. Pharm. Sci.* **1995**, *84*, 983.
(14) Shambling, S. L.; Tang, X.; Chang, L.; Hancock, B. C.; Pikal, M. J. *J. Phys. Chem. B* **1999**, *103*, 4113.
(15) Alie, J.; Menegotto, J.; Cardon, P.; Duplaa, H.; Caron, A.; Lacabanne, C.; Bauer, M. *J. Pharm. Sci.* **2004**, *93*, 218.
(16) Johari, G. P.; Kim, S.; Shanker, R. M. *J. Pharm. Sci.* **2005**, *94*, 2207.
(17) Descamps, M.; Correia, N. T.; Derollez, P.; Danede, F.; Capet, F. *J. Phys. Chem. B* **2005**, *109*, 16092.
(18) Carpentier, L.; Decressain, R.; De Gusseme, A.; Neves, C.; Descamps, M. *Pharm. Res.* **2006**, *23*, 798.
(19) Carpentier, L.; Decressain, R.; Desprez, S.; Descamps, M. *J. Phys. Chem. B* **2006**, *110*, 457.
(20) Nath, R.; El Goresy, T.; Geil, B.; Zimmermann, H.; Böhmer, R. *Phys. Rev. E.* **2006**, *74*, 021506.
(21) Kamiński, K.; Paluch, M.; Ziolo, J.; Ngai, K. L. *J. Phys.:Condens. Matter* **2006**, *18*, 5607.
(22) El Goresy, T.; Böhmer, R. *J. Phys.:Condens. Matter* **2007**, *19*, 205134.
(23) (a) The T_g scaled viscosity plot that is in the origin of the fragility concept was originally given by: Laughlin, W. T.; Uhlmann, D. R *J. Phys. Chem.* **1972**, *76*, 2317. (b) Oldekop, W. *Glasstech. Ber.* **1957**, *30*, 8. (c) Revised in: Ngai, K. L. *J. Non-Cryst. Solids* **2000**, *275*, 7.
(24) Angell, C. A., *In Relaxations in Complex Systems*; Ngai, K. L.; Wright, G. B., Eds.; National Technical Information Service, US Department of Commerce, Springfield, VA, 1985; p 1.
(25) Angell, C. A. *J. Non-Cryst. Solids* **1991**, *131−133*, 13. Angell, C. A. *J. Res. Natl. Inst. Stand. Technol.* **1997**, *102*, 171.
(26) Kremer, F., Schönhals, A., Eds. *Broadband Dielectric Spectroscopy*; Springer Verlag: Berlin, 2002.
(27) Craig, D. Q. M. *Dielectric Analysis of Pharmaceutical Systems*; Taylor & Francis: London, 1995.
(28) Huth, H.; Wang, L.-M.; Schick, C.; Richert, R. *J. Chem. Phys.* **2007**, *126*, 104503–1.
(29) Moura Ramos, J. J.; Correia, N. T.; Diogo, H. P. *Phys. Chem. Chem. Phys.* **2004**, *6*, 793.
(30) Lerdkanchanaporn, S.; Dollimore, D. *J. Therm. Anal.* **1997**, *49*, 879.
(31) Romero, A. J.; Savastano, L.; Rhodes, C. T *Int. J. Pharm.* **1993**, *99*, 125.
(32) (a) Havriliak, S.; Negami, S. *Polymer* **1967**, *8*, 161. Havriliak, S.; Negami, S. *J. Polym. Sci. C* **1966**, *16*, 99. (b) Recently revised in: Havriliak, S., Jr., Havriliak, S., *Dielectric and Mechanical Relaxation in Material*, Hanser: Munich, Germany, 1997.
(33) Schönhals, A.; Kremer, F. In Analysis of Dielectric Spectra. *Broadband Dielectric Spectroscopy*; Kremer, F., Schönhals, A., Eds.; Springer Verlag: Berlin, 2002; Chapter 3.
(34) Hartmann, L.; Kremer, F.; Pouret, P.; Léger, L. *J. Chem. Phys.* **2003**, *118*, 6052.
(35) *The dlpoly user manual*; Smith, W., Forester, T. R., Eds.; CCLRC, Daresbury Laboratory; Warrington, England, 2001.
(36) Wang, J.; Wolf, R. M.; Caldwell, J. W.; Kollman, P. A.; Case, D. A. *J. Comput. Chem.* **2004**, *25*, 1157.
(37) Shankland, N.; Wilson, C. C.; Florence, A. J.; Cox, P. C. *Acta Crystallogr.* **1997**, *C53*, 951.
(38) Ryckaert, J. P.; Ciccotti, G.; Berendsen, H. J. C. *J. Comput. Phys.* **1977**, *23*, 327.
(39) Hockney, R. W. *Meth. Comp. Phys.* **1970**, *9*, 136.
(40) Frisch, M. J.; Trucks, G. W.; Schlegel, H. B.; Scuseria, G. E.; Robb, M. A.; Cheeseman, J. R.; Zakrzewski, V. G.; Montgomery, J. A.; Stratmann, R. E; Burant, J. C.; Dapprich, S.; Millam, J. M.; Daniels, A.; Kudin, K. N.; Strain, M. C.; Farkas, O.; Tomasi, J.; Barone, V.; Cossi, M.; Cammi, R.; Mennucci, B.; Pomelli, C.; Adamo, C.; Clifford, S.; Ochterski, J.; Petersson, G. A.; Ayala, P. Y.; Cui, Q.; Morokuma, K.; Malick, D. K.; Rabuck, A. D.; Raghavachari, K.; Foresman, J. B.; Cioslowski, J.; Ortiz, J. V.; Stefanov, B. B.; Liu, G.; Liashenko, A.; Piskorz, P.; Komaromi, I.; Gomperts, R.; Martin, R. L.; Fox, D. J.; Keith, T.; Al-Laham, M. A.; Peng, C. Y.; Nanayakkara, A.; Gonzalez, C.; Challacombe, M.; Gill, P. M. W.; Johnson, B.; Chen, W.; Wong, M. W.; Andres, J. L.; Head-Gordon, M.; Replogle, E. S.; Pople, J. A.; *Gaussian98, revision a.7*. Gaussian, Inc.: Pittsburgh, PA, 1998.
(41) Vueba, M. L.; Pina, M. E.; de Carvalho, L. A. E. B. *J. Pharm. Sci.* **2007**, *97*, 834.
(42) Berendsen, H. J. C.; Postma, J. P. M.; van Gunsteren, W. F.; DiNola, A.; Haak, J. R. *J. Chem. Phys.* **1984**, *81*, 3684.
(43) Schug, K.; McNair, H. M. *J. Sep. Sci.* **2002**, *25*, 760.
(44) Loo, J. A. *Mass Spectrom. Rev.* **1997**, *16*, 1.
(45) Koshy, K. M.; Boggs, J. M *J. Biol. Chem.* **1996**, *271*, 3496.
(46) Schug, K.; McNair, H. M. *J. Chromatogr. A* **2003**, *985*, 531.
(47) Silverstein, R. M.; Bassler, G. C.; Morril, T. C. *Spectrometric identification of organic compounds*, 5th Ed.; John Wiley & Sons: New York, 1991.
(48) Dong, J.; Ozaki, Y.; Nakashima, K. *Macromolecules* **1997**, *30*, 1111.
(49) Setoguchi, Y.; Monobe, H.; Wan, W.; Terasawa, N.; Kiyohara, K.; Nakamura, N.; Shimizu, Y. *Mol. Cryst. Liq. Crys.* **2004**, *412*, 9.
(50) McConnell, J. F. *Cryst. Struct. Commun.* **1974**, *3*, 73–75.
(51) Liu, Q.; Schmidt, R. K.; Teo, B.; Karplus, P. A.; Brady, J. W. *J. Am. Chem. Soc.* **1997**, *119*, 7851.
(52) Saiz, L.; Padro, J. A.; Guardia, E. *Mol. Phys.* **1999**, *97*, 897.
(53) Hansen, L. K.; Perlovich, G. L.; Bauer-Brandl, A. *Acta Crystallogr.* **2003**, *E59*, o1357.
(54) Hansen, L. K.; Perlovich, G. L.; Bauer-Brandl, A. *Acta Crystallogr.* **2006**, *E62*, e17.
(55) Pal, S.; Bagchi, B.; Balasubramanian, S. *J. Phys. Chem. B* **2005**, *109*, 12879.
(56) Xu, F.; Sun, L.-X.; Tan, Z.-C.; Liang, J.-G.; Li, R.-L. *Thermochim. Acta* **2004**, *412*, 33.

(57) Dudognon, E.; Dañede, F.; Descamps, M.; Correia, N. T. *Pharm. Res.* **2008**; DOI 10.1007/s11095−998−9655−7.
(58) Kohlrausch, R. *Pogg. Ann. Phys. III* **1847**, *12*, 393.
(59) Williams, G.; Watts, D. C. *Trans. Faraday. Soc.* **1966**, *66*, 80.
(60) Alvarez, F.; Alegría, A.; Colmenero, J. *Phys. Rev. B* **1991**, *44*, 7306.
(61) (a) Böttcher; C. J. F. ; *Theory of Dielectric Polarization*; Elsevier: Amsterdam 1973; Vol. 1. (b) Böttcher; C. J. F.; Bordewijk, P.; *Theory of Dielectric Polarization*; Elsevier: Amsterdam; 1978; Vol. 2.
(62) Hansen, C.; Stickel, F.; Berger, T.; Richert, R.; Fischer, E. W. *J. Chem. Phys.* **1997**, *107*, 1086.
(63) Ngai, K. L.; Paluch, M. *J. Chem. Phys.* **2004**, *120*, 857.
(64) Wagner, H.; Richert, R. *J. Phys. Chem. B* **1999**, *103*, 4071.
(65) Döss, A.; Paluch, M.; Sillescu, H.; Hinze, G. *Phys. Rev. Lett.* **2002**, *88*, 095701.
(66) Casalini, R.; Fioretto, D.; Livi, A.; Lucchesi, M.; Rolla, P. A. *Phys. Rev. B* **1997**, *56*, 3016.
(67) Smith, I. K.; Andrews, S. R.; Williams, G.; Holmesb, P. A. *J. Mater. Chem.* **1997**, *7*, 203.
(68) Viciosa, M. T.; Rodrigues, C.; Fernández, S.; Matos, I.; Marques, M. M.; Duarte, M. T.; Mano, J. F.; Dionísio, M. *J. Polym. Sci.: Part B: Polym. Phys.* **2007**, *45*, 2802.
(69) Kaminska, E.; Kaminski, K.; Hensel-Bielowka, S.; Paluch, M.; Ngai, K. L. *J. Non-Cryst. Solids* **2006**, *352*, 4672.
(70) Corezzi, S.; Beiner, M.; Huth, H.; Schröter, K.; Capaccioli, S.; Casalini, R.; Fioretto, D.; Donth, E. *J. Chem. Phys.* **2002**, *117*, 2435.
(71) Paluch, M.; Roland, C. M.; Pawlus, S.; Ziolo, J.; Ngai, K. L. *Phys. Rev. Lett.* **2003**, *91*, 115701.
(72) Capaccioli, S.; Kessairi, K.; Prevosto, D.; Lucchesi, M.; Ngai, K. L. *J. Non-Cryst. Solids* **2006**, *352*, 4643.
(73) Capaccioli, S.; Kessairi, K.; Prevosto, D.; Lucchesi, M.; Rolla, P. A. *J. Phys.: Condens. Matter* **2007**, *19*, 205133.
(74) Ngai, K. L. J. *Phys.: Condens. Matter* **2003**, *15*, S1107.
(75) Ngai, K. L.; Kamińska, E.; Sekula, M.; Paluch, M. *J. Chem. Phys.* **2005**, *123*, 204507.
(76) Johari, G. P.; Goldstein, M. *J. Chem. Phys.* **1970**, *53*, 2372 J. Chem. Phys. **1971**, 55, 4245.
(77) Ngai, K. L.; Capaccioli, S. *Phys. Rev. E* **2004**, *69*, 031051.
(78) Kudlik, A.; Tschirwitz, C.; Blochowicz, T.; Benkhof, S.; Rössler, E. *J. Non-Cryst. Solids* **1998**, *235−237*, 406.
(79) Wang, L.-M.; Richert, R. *Phys. Rev. B* **2007**, *76*, 064201.
(80) Nozaki, R.; Zenitani, H.; Minoguchi, A.; Kitai, K. *J. Non-Cryst. Solids* **2002**, *307−310*, 349.
(81) Nath, R.; Nowaczyk, A.; Geil, B.; Böhmer, R. *J. Non-Cryst. Solids* **2007**, *353*, 3788.
(82) Berg, O. v; d, Wübbenhorst, M.; Picken, S. J.; Jager, W. F. *J. Non-Cryst. Solids* **2005**, *351*, 2694.
(83) Vogel, H. *Phys. Zeit.* **1921**, *22*, 645.
(84) Fulcher, G. S. *J. Am. Ceram. Soc.* **1925**, *8*, 339.
(85) Tammann, G.; Hesse, G. Z. *Anorg. Allg. Chem.* **1926**, *156*, 245.
(86) Donth, E. *The Glass Transition*; Springer Verlag: Berlin, 2001.
(87) Schönhals, A.; Kremer, F. In *The scaling of the dynamics of glasses and supercooled liquids. In Broadband Dielectric Spectroscopy*; Kremer, F., Schönhals, A., Eds.; Springer Verlag: Berlin, 2002; Chapter 4 and references therein.
(88) Stickel, F.; Fischer, E. W.; Richert, R. *J. Chem. Phys.* **1996**, *104*, 2043.
(89) Schönhals, A.; Schick, Ch.; Huth, H.; Frick, B.; Mayorova, M.; Zorn, R. *J. Non-Cryst. Solids* **2007**, *353*, 3853.
(90) Schönhals, A. Molecular Dynamics in Polymer Model Systems In *Broadband Dielectric Spectroscopy*; Kremer, F., Schönhals, A., Eds.; Springer Verlag: Berlin, 2002; Chapter 7.
(91) Ngai, K. L.; Roland, C. M. *Polymer* **2002**, *43*, 567.
(92) Wang, L.-M.; Richert, R. J. *Chem. Phys.* **2004**, *121*, 11170.
(93) Tyagi, M.; Alegria, A.; Colmenero, J. *J. Chem. Phys.* **2005**, *122*, 244909.
(94) Böhmer, R.; Ngai, K. L.; Angell, C. A.; Plazek, D. J. *J. Chem. Phys.* **1993**, *99*, 4201.
(95) Wang, L.-M.; Richert, R. *J. Phys. Chem. B Lett.* **2005**, *109*, 1091.
(96) Paleos, C.; Tsiourvas, D. *Liquid Cryst.* **2001**, *28*, 1127.
(97) Chen, W.; Wunderlich, B. *Macromol. Chem. Phys.* **1999**, *200*, 283.
(98) Moura Ramos, J. J.; Diogo, H. P.; Godinho, M. H.; Cruz, C.; Merkel, K. *J. Phys. Chem. B* **2004**, *108*, 7955.

JP8040428